Search for a Fermiophobic and Standard Model Higgs Boson in Diphoton Final States

V. M. Abazov,[35] B. Abbott,[73] B. S. Acharya,[29] M. Adams,[49] T. Adams,[47] G. D. Alexeev,[35] G. Alkhazov,[39] A. Alton,[61,†]
G. Alverson,[60] G. A. Alves,[2] M. Aoki,[48] M. Arov,[58] A. Askew,[47] B. Åsman,[41] O. Atramentov,[65] C. Avila,[8]
J. BackusMayes,[80] F. Badaud,[13] L. Bagby,[48] B. Baldin,[48] D. V. Bandurin,[47] S. Banerjee,[29] E. Barberis,[60] P. Baringer,[56]
J. Barreto,[3] J. F. Bartlett,[48] U. Bassler,[18] V. Bazterra,[49] S. Beale,[6] A. Bean,[56] M. Begalli,[3] M. Begel,[71]
C. Belanger-Champagne,[41] L. Bellantoni,[48] S. B. Beri,[27] G. Bernardi,[17] R. Bernhard,[22] I. Bertram,[42] M. Besançon,[18]
R. Beuselinck,[43] V. A. Bezzubov,[38] P. C. Bhat,[48] V. Bhatnagar,[27] G. Blazey,[50] S. Blessing,[47] K. Bloom,[64] A. Boehnlein,[48]
D. Boline,[70] E. E. Boos,[37] G. Borissov,[42] T. Bose,[59] A. Brandt,[76] O. Brandt,[23] R. Brock,[62] G. Brooijmans,[68] A. Bross,[48]
D. Brown,[17] J. Brown,[17] X. B. Bu,[48] M. Buehler,[79] V. Buescher,[24] V. Bunichev,[37] S. Burdin,[42,‡] T. H. Burnett,[80]
C. P. Buszello,[41] B. Calpas,[15] E. Camacho-Pérez,[32] M. A. Carrasco-Lizarraga,[56] B. C. K. Casey,[48] H. Castilla-Valdez,[32]
S. Chakrabarti,[70] D. Chakraborty,[50] K. M. Chan,[54] A. Chandra,[78] G. Chen,[56] S. Chevalier-Théry,[18] D. K. Cho,[75]
S. W. Cho,[31] S. Choi,[31] B. Choudhary,[28] S. Cihangir,[48] D. Claes,[64] J. Clutter,[56] M. Cooke,[48] W. E. Cooper,[48]
M. Corcoran,[78] F. Couderc,[18] M.-C. Cousinou,[15] A. Croc,[18] D. Cutts,[75] A. Das,[45] G. Davies,[43] K. De,[76] S. J. de Jong,[34]
E. De La Cruz-Burelo,[32] F. Déliot,[18] M. Demarteau,[48] R. Demina,[69] D. Denisov,[48] S. P. Denisov,[38] S. Desai,[48] C. Deterre,[18]
K. DeVaughan,[64] H. T. Diehl,[48] M. Diesburg,[48] P. F. Ding,[44] A. Dominguez,[64] T. Dorland,[80] A. Dubey,[28] L. V. Dudko,[37]
D. Duggan,[65] A. Duperrin,[15] S. Dutt,[27] A. Dyshkant,[50] M. Eads,[64] D. Edmunds,[62] J. Ellison,[46] V. D. Elvira,[48] Y. Enari,[17]
H. Evans,[52] A. Evdokimov,[71] V. N. Evdokimov,[38] G. Facini,[60] T. Ferbel,[69] F. Fiedler,[24] F. Filthaut,[34] W. Fisher,[62]
H. E. Fisk,[48] M. Fortner,[50] H. Fox,[42] S. Fuess,[48] A. Garcia-Bellido,[69] V. Gavrilov,[36] P. Gay,[13] W. Geng,[15,62] D. Gerbaudo,[66]
C. E. Gerber,[49] Y. Gershtein,[65] G. Ginther,[48,69] G. Golovanov,[35] A. Goussiou,[80] P. D. Grannis,[70] S. Greder,[19] H. Greenlee,[48]
Z. D. Greenwood,[58] E. M. Gregores,[4] G. Grenier,[20] Ph. Gris,[13] J.-F. Grivaz,[16] A. Grohsjean,[18] S. Grünendahl,[48]
M. W. Grünewald,[30] T. Guillemin,[16] F. Guo,[70] G. Gutierrez,[48] P. Gutierrez,[73] A. Haas,[68,§] S. Hagopian,[47] J. Haley,[60]
L. Han,[7] K. Harder,[44] A. Harel,[69] J. M. Hauptman,[55] J. Hays,[43] T. Head,[44] T. Hebbeker,[21] D. Hedin,[50] H. Hegab,[74]
A. P. Heinson,[46] U. Heintz,[75] C. Hensel,[23] I. Heredia-De La Cruz,[32] K. Herner,[61] G. Hesketh,[44,‖] M. D. Hildreth,[54]
R. Hirosky,[79] T. Hoang,[47] J. D. Hobbs,[70] B. Hoeneisen,[12] M. Hohlfeld,[24] Z. Hubacek,[10,18] N. Huske,[17] V. Hynek,[10]
I. Iashvili,[67] Y. Ilchenko,[77] R. Illingworth,[48] A. S. Ito,[48] S. Jabeen,[75] M. Jaffré,[16] D. Jamin,[15] A. Jayasinghe,[73] R. Jesik,[43]
K. Johns,[45] M. Johnson,[48] D. Johnston,[64] A. Jonckheere,[48] P. Jonsson,[43] J. Joshi,[27] A. W. Jung,[48] A. Juste,[40] K. Kaadze,[57]
E. Kajfasz,[15] D. Karmanov,[37] P. A. Kasper,[48] I. Katsanos,[64] R. Kehoe,[77] S. Kermiche,[15] N. Khalatyan,[48] A. Khanov,[74]
A. Kharchilava,[67] Y. N. Kharzheev,[35] M. H. Kirby,[51] J. M. Kohli,[27] A. V. Kozelov,[38] J. Kraus,[62] S. Kulikov,[38] A. Kumar,[67]
A. Kupco,[11] T. Kurča,[20] V. A. Kuzmin,[37] J. Kvita,[9] S. Lammers,[52] G. Landsberg,[75] P. Lebrun,[20] H. S. Lee,[31] S. W. Lee,[55]
W. M. Lee,[48] J. Lellouch,[17] L. Li,[46] Q. Z. Li,[48] S. M. Lietti,[5] J. K. Lim,[31] D. Lincoln,[48] J. Linnemann,[62] V. V. Lipaev,[38]
R. Lipton,[48] Y. Liu,[7] Z. Liu,[6] A. Lobodenko,[39] M. Lokajicek,[11] R. Lopes de Sa,[70] H. J. Lubatti,[80] R. Luna-Garcia,[32,¶]
A. L. Lyon,[48] A. K. A. Maciel,[2] D. Mackin,[78] R. Madar,[18] R. Magaña-Villalba,[32] S. Malik,[64] V. L. Malyshev,[35]
Y. Maravin,[57] J. Martínez-Ortega,[32] R. McCarthy,[70] C. L. McGivern,[56] M. M. Meijer,[34] A. Melnitchouk,[63] D. Menezes,[50]
P. G. Mercadante,[4] M. Merkin,[37] A. Meyer,[21] J. Meyer,[23] F. Miconi,[19] N. K. Mondal,[29] G. S. Muanza,[15] M. Mulhearn,[79]
E. Nagy,[15] M. Naimuddin,[28] M. Narain,[75] R. Nayyar,[28] H. A. Neal,[61] J. P. Negret,[8] P. Neustroev,[39] S. F. Novaes,[5]
T. Nunnemann,[25] G. Obrant,[39,*] J. Orduna,[78] N. Osman,[15] J. Osta,[54] G. J. Otero y Garzón,[1] M. Padilla,[46] A. Pal,[76]
N. Parashar,[53] V. Parihar,[75] S. K. Park,[31] J. Parsons,[68] R. Partridge,[75,§] N. Parua,[52] A. Patwa,[71] B. Penning,[48] M. Perfilov,[37]
K. Peters,[44] Y. Peters,[44] K. Petridis,[44] G. Petrillo,[69] P. Pétroff,[16] R. Piegaia,[1] M.-A. Pleier,[71] P. L. M. Podesta-Lerma,[32,**]
V. M. Podstavkov,[48] P. Polozov,[36] A. V. Popov,[38] M. Prewitt,[78] D. Price,[52] N. Prokopenko,[38] S. Protopopescu,[71] J. Qian,[61]
A. Quadt,[23] B. Quinn,[63] M. S. Rangel,[2] K. Ranjan,[28] P. N. Ratoff,[42] I. Razumov,[38] P. Renkel,[77] M. Rijssenbeek,[70]
I. Ripp-Baudot,[19] F. Rizatdinova,[74] M. Rominsky,[48] A. Ross,[42] C. Royon,[18] P. Rubinov,[48] R. Ruchti,[54] G. Safronov,[36]
G. Sajot,[14] P. Salcido,[50] A. Sánchez-Hernández,[32] M. P. Sanders,[25] B. Sanghi,[48] A. S. Santos,[5] G. Savage,[48] L. Sawyer,[58]
T. Scanlon,[43] R. D. Schamberger,[70] Y. Scheglov,[39] H. Schellman,[51] T. Schliephake,[26] S. Schlobohm,[80]
C. Schwanenberger,[44] R. Schwienhorst,[62] J. Sekaric,[56] H. Severini,[73] E. Shabalina,[23] V. Shary,[18] A. A. Shchukin,[38]
R. K. Shivpuri,[28] V. Simak,[10] V. Sirotenko,[48] P. Skubic,[73] P. Slattery,[69] D. Smirnov,[54] K. J. Smith,[67] G. R. Snow,[64]
J. Snow,[72] S. Snyder,[71] S. Söldner-Rembold,[44] L. Sonnenschein,[21] K. Soustruznik,[9] J. Stark,[14] V. Stolin,[36]
D. A. Stoyanova,[38] M. Strauss,[73] D. Strom,[49] L. Stutte,[48] L. Suter,[44] P. Svoisky,[73] M. Takahashi,[44] A. Tanasijczuk,[1]
W. Taylor,[6] M. Titov,[18] V. V. Tokmenin,[35] Y.-T. Tsai,[69] D. Tsybychev,[70] B. Tuchming,[18] C. Tully,[66] L. Uvarov,[39]
S. Uvarov,[39] S. Uzunyan,[50] R. Van Kooten,[52] W. M. van Leeuwen,[33] N. Varelas,[49] E. W. Varnes,[45] I. A. Vasilyev,[38]

0031-9007/11/107(15)/151801(7)

P. Verdier,[20] L. S. Vertogradov,[35] M. Verzocchi,[48] M. Vesterinen,[44] D. Vilanova,[18] P. Vokac,[10] H. D. Wahl,[47] M. H. L. S. Wang,[48] J. Warchol,[54] G. Watts,[80] M. Wayne,[54] M. Weber,[48,††] L. Welty-Rieger,[51] A. White,[76] D. Wicke,[26] M. R. J. Williams,[42] G. W. Wilson,[56] M. Wobisch,[58] D. R. Wood,[60] T. R. Wyatt,[44] Y. Xie,[48] C. Xu,[61] S. Yacoob,[51] R. Yamada,[48] W.-C. Yang,[44] T. Yasuda,[48] Y. A. Yatsunenko,[35] Z. Ye,[48] H. Yin,[48] K. Yip,[71] S. W. Youn,[48] J. Yu,[76] S. Zelitch,[79] T. Zhao,[80] B. Zhou,[61] J. Zhu,[61] M. Zielinski,[69] D. Zieminska,[52] and L. Zivkovic[75]

(D0 Collaboration)

[1]*Universidad de Buenos Aires, Buenos Aires, Argentina*
[2]*LAFEX, Centro Brasileiro de Pesquisas Físicas, Rio de Janeiro, Brazil*
[3]*Universidade do Estado do Rio de Janeiro, Rio de Janeiro, Brazil*
[4]*Universidade Federal do ABC, Santo André, Brazil*
[5]*Instituto de Física Teórica, Universidade Estadual Paulista, São Paulo, Brazil*
[6]*Simon Fraser University, Vancouver, British Columbia, and York University, Toronto, Ontario, Canada*
[7]*University of Science and Technology of China, Hefei, People's Republic of China*
[8]*Universidad de los Andes, Bogotá, Colombia*
[9]*Charles University, Faculty of Mathematics and Physics, Center for Particle Physics, Prague, Czech Republic*
[10]*Czech Technical University in Prague, Prague, Czech Republic*
[11]*Center for Particle Physics, Institute of Physics, Academy of Sciences of the Czech Republic, Prague, Czech Republic*
[12]*Universidad San Francisco de Quito, Quito, Ecuador*
[13]*LPC, Université Blaise Pascal, CNRS/IN2P3, Clermont, France*
[14]*LPSC, Université Joseph Fourier Grenoble 1, CNRS/IN2P3, Institut National Polytechnique de Grenoble, Grenoble, France*
[15]*CPPM, Aix-Marseille Université, CNRS/IN2P3, Marseille, France*
[16]*LAL, Université Paris-Sud, CNRS/IN2P3, Orsay, France*
[17]*LPNHE, Universités Paris VI and VII, CNRS/IN2P3, Paris, France*
[18]*CEA, Irfu, SPP, Saclay, France*
[19]*IPHC, Université de Strasbourg, CNRS/IN2P3, Strasbourg, France*
[20]*IPNL, Université Lyon 1, CNRS/IN2P3, Villeurbanne, France and Université de Lyon, Lyon, France*
[21]*III. Physikalisches Institut A, RWTH Aachen University, Aachen, Germany*
[22]*Physikalisches Institut, Universität Freiburg, Freiburg, Germany*
[23]*II. Physikalisches Institut, Georg-August-Universität Göttingen, Göttingen, Germany*
[24]*Institut für Physik, Universität Mainz, Mainz, Germany*
[25]*Ludwig-Maximilians-Universität München, München, Germany*
[26]*Fachbereich Physik, Bergische Universität Wuppertal, Wuppertal, Germany*
[27]*Panjab University, Chandigarh, India*
[28]*Delhi University, Delhi, India*
[29]*Tata Institute of Fundamental Research, Mumbai, India*
[30]*University College Dublin, Dublin, Ireland*
[31]*Korea Detector Laboratory, Korea University, Seoul, Korea*
[32]*CINVESTAV, Mexico City, Mexico*
[33]*Nikhef, Science Park, Amsterdam, The Netherlands*
[34]*Radboud University Nijmegen, Nijmegen, The Netherlands and Nikhef, Science Park, Amsterdam, The Netherlands*
[35]*Joint Institute for Nuclear Research, Dubna, Russia*
[36]*Institute for Theoretical and Experimental Physics, Moscow, Russia*
[37]*Moscow State University, Moscow, Russia*
[38]*Institute for High Energy Physics, Protvino, Russia*
[39]*Petersburg Nuclear Physics Institute, St. Petersburg, Russia*
[40]*Institució Catalana de Recerca i Estudis Avançats (ICREA) and Institut de Física d'Altes Energies (IFAE), Barcelona, Spain*
[41]*Stockholm University, Stockholm and Uppsala University, Uppsala, Sweden*
[42]*Lancaster University, Lancaster LA1 4YB, United Kingdom*
[43]*Imperial College London, London SW7 2AZ, United Kingdom*
[44]*The University of Manchester, Manchester M13 9PL, United Kingdom*
[45]*University of Arizona, Tucson, Arizona 85721, USA*
[46]*University of California Riverside, Riverside, California 92521, USA*
[47]*Florida State University, Tallahassee, Florida 32306, USA*
[48]*Fermi National Accelerator Laboratory, Batavia, Illinois 60510, USA*
[49]*University of Illinois at Chicago, Chicago, Illinois 60607, USA*
[50]*Northern Illinois University, DeKalb, Illinois 60115, USA*
[51]*Northwestern University, Evanston, Illinois 60208, USA*

[52]*Indiana University, Bloomington, Indiana 47405, USA*
[53]*Purdue University Calumet, Hammond, Indiana 46323, USA*
[54]*University of Notre Dame, Notre Dame, Indiana 46556, USA*
[55]*Iowa State University, Ames, Iowa 50011, USA*
[56]*University of Kansas, Lawrence, Kansas 66045, USA*
[57]*Kansas State University, Manhattan, Kansas 66506, USA*
[58]*Louisiana Tech University, Ruston, Louisiana 71272, USA*
[59]*Boston University, Boston, Massachusetts 02215, USA*
[60]*Northeastern University, Boston, Massachusetts 02115, USA*
[61]*University of Michigan, Ann Arbor, Michigan 48109, USA*
[62]*Michigan State University, East Lansing, Michigan 48824, USA*
[63]*University of Mississippi, University, Mississippi 38677, USA*
[64]*University of Nebraska, Lincoln, Nebraska 68588, USA*
[65]*Rutgers University, Piscataway, New Jersey 08855, USA*
[66]*Princeton University, Princeton, New Jersey 08544, USA*
[67]*State University of New York, Buffalo, New York 14260, USA*
[68]*Columbia University, New York, New York 10027, USA*
[69]*University of Rochester, Rochester, New York 14627, USA*
[70]*State University of New York, Stony Brook, New York 11794, USA*
[71]*Brookhaven National Laboratory, Upton, New York 11973, USA*
[72]*Langston University, Langston, Oklahoma 73050, USA*
[73]*University of Oklahoma, Norman, Oklahoma 73019, USA*
[74]*Oklahoma State University, Stillwater, Oklahoma 74078, USA*
[75]*Brown University, Providence, Rhode Island 02912, USA*
[76]*University of Texas, Arlington, Texas 76019, USA*
[77]*Southern Methodist University, Dallas, Texas 75275, USA*
[78]*Rice University, Houston, Texas 77005, USA*
[79]*University of Virginia, Charlottesville, Virginia 22901, USA*
[80]*University of Washington, Seattle, Washington 98195, USA*
(Received 22 July 2011; published 5 October 2011)

We present a search for the standard model Higgs boson and a fermiophobic Higgs boson in the diphoton final states based on 8.2 fb^{-1} of $p\bar{p}$ collisions at $\sqrt{s} = 1.96$ TeV collected with the D0 detector at the Fermilab Tevatron Collider. No excess of data above background predictions is observed and upper limits at the 95% C.L. on the cross section multiplied by the branching fraction are set which are the most restrictive to date. A fermiophobic Higgs boson with a mass below 112.9 GeV is excluded at the 95% C.L.

DOI: 10.1103/PhysRevLett.107.151801 PACS numbers: 14.80.Bn, 12.60.Fr, 13.85.Rm, 14.80.Ec

In the standard model (SM), the Higgs boson (H) is the last undiscovered particle that provides crucial insights on the spontaneous breaking of the electroweak symmetry and the generation of mass of the weak gauge bosons and fermions. The constraints from the direct searches at the CERN e^+e^- Collider (LEP) [1] and from the measurement of precision electroweak observables [2] result in a preferred range for the SM Higgs boson mass of $114.4 < M_H < 185$ GeV at 95% C.L. Furthermore, the range $158 < M_H < 173$ GeV is excluded at 95% C.L. by the direct searches at the Fermilab Tevatron $p\bar{p}$ Collider [3]. These experimental constraints are derived assuming SM production and decay modes for the Higgs boson and can be substantially modified in case of significant departures from the SM.

At hadron colliders the dominant production mechanisms for a light SM Higgs boson are gluon fusion (GF) ($gg \to H$), associated production with a W or Z boson ($q\bar{q}' \to VH$, $V = W, Z$), and vector boson fusion (VBF) ($VV \to H$). At the Tevatron, the most sensitive SM Higgs boson searches rely on the $VH(H \to b\bar{b})$ process for $M_H < 125$ GeV and on $gg \to H \to W^+W^-$ for $M_H > 125$ GeV. At CERN's Large Hadron Collider (LHC), the strategy at high M_H (> 140 GeV) is similar, while at low M_H (< 140 GeV) the $H \to \gamma\gamma$ decay mode becomes one of the most promising discovery channels, despite its small branching ratio of $\mathcal{B}(H \to \gamma\gamma) \approx 0.2\%$ for $110 < M_H < 140$ GeV, owing to its clean experimental signature of a narrow resonance on top of a smoothly falling background in the diphoton mass spectrum. Some of the most sensitive searches for the SM Higgs boson involve the loop-mediated ggH and/or $\gamma\gamma H$ vertices, which are also sensitive to new physics effects. For instance, the addition of a sequential fourth family of quarks can substantially enhance the ggH coupling, leading to an increase in the GF production rate, while decreasing $\mathcal{B}(H \to b\bar{b})$ [4]. Alternatively, other models of electroweak symmetry breaking can involve suppressed couplings to some or all fermions [5]. The extreme case is the fermiophobic Higgs boson (H_f) model, in which H_f has no tree-level coupling to fermions but standard coupling to bosons, resulting in only VH and VBF production and a significantly enhanced $\mathcal{B}(H_f \to \gamma\gamma)$. Thus, Higgs boson searches in the $\gamma\gamma$ decay mode can be a sensitive probe of new physics models where the Higgs boson may be difficult to observe in other, *a priori* more promising, channels.

This Letter presents a search for a Higgs boson decaying into $\gamma\gamma$ using an inclusive diphoton sample collected with the D0 detector in $p\bar{p}$ collisions at $\sqrt{s} = 1.96$ TeV at the Fermilab Tevatron Collider. In this search both the SM and the fermiophobic Higgs boson models are considered. The most recent searches at the Tevatron for a SM Higgs boson [6] or a fermiophobic Higgs boson [7] in the $\gamma\gamma$ mode analyzed the diphoton invariant mass spectrum in search for a narrow resonance. This analysis represents a significant step forward in sensitivity by increasing the data set by nearly a factor of 3, as well as by exploiting further kinematic differences between signal and background through a multivariate analysis technique.

The D0 detector is described in detail elsewhere [8]. The subdetectors most relevant to this analysis are the central tracking system, composed of a silicon microstrip tracker (SMT) and a central fiber tracker (CFT) in a 2 T solenoidal magnetic field, the central preshower (CPS), and the liquid-argon and uranium sampling calorimeter. The CPS is located immediately before the inner layer of the calorimeter and is formed by one radiation length of absorber followed by several layers of scintillating strips. The calorimeter consists of three sections housed in separate cryostats: a central section covering up to $|\eta| \approx 1.1$ [9] and two end calorimeters extending the coverage up to $|\eta| \approx 4.2$. They are divided into electromagnetic (EM) and hadronic layers. The EM section of the calorimeter is segmented into four longitudinal layers with transverse segmentation of $\Delta\eta \times \Delta\phi = 0.1 \times 0.1$ [9], except in the third layer (EM3), where it is 0.05×0.05. The calorimeter is well suited for a precise measurement of electron and photon energies, providing a resolution of $\approx 3.6\%$ at electron and photon energies of ≈ 50 GeV. The data used in this analysis were collected using triggers requiring at least two clusters of energy in the EM calorimeter and correspond to an integrated luminosity of 8.2 fb^{-1} [10].

Events are selected by requiring at least two photon candidates with transverse momentum $p_T > 25$ GeV in the central region of the calorimeter ($|\eta| < 1.1$), for which the trigger requirements are close to 100% efficient. Photon candidates are selected from EM clusters reconstructed with a simple cone algorithm with radius $\mathcal{R} = \sqrt{(\Delta\eta)^2 + (\Delta\phi)^2} = 0.2$ that satisfy the following requirements: (i) at least 95% of the cluster energy is deposited in the EM calorimeter; (ii) the calorimeter isolation variable $I = [E_{\rm tot}(0.4) - E_{\rm EM}(0.2)]/E_{\rm EM}(0.2)$ is less than 0.1, where $E_{\rm tot}(0.4)$ is the total energy in a cone of radius $\mathcal{R} = 0.4$ and $E_{\rm EM}(0.2)$ is the EM energy in a cone of radius $\mathcal{R} = 0.2$; (iii) the energy-weighted cluster width in EM3 is consistent with an EM shower [11]; (iv) the scalar sum of the p_T of all tracks originating from the primary $p\bar{p}$ interaction vertex in an annulus of $0.05 < \mathcal{R} < 0.4$ around the cluster is less than 2 GeV; (v) the EM cluster is not spatially matched to tracker activity, either to a reconstructed track, or to a set of hits in the SMT and CFT consistent with that of an electron or positron trajectory [12]; and (vi) the output of a photon neural network ($O_{\rm NN}$) [6,13], combining information from a set of variables that are sensitive to differences between photons and jets in the tracker, the calorimeter and the CPS, is larger than 0.1. Requirement (v) is intended to reject electrons but converted photons are mostly removed as well. Requirement (vi) rejects approximately 40% of the misidentified jets, while keeping >98% of real photons. Finally, additional kinematic selections are applied in order to select a signal-enriched sample. The diphoton invariant mass, $M_{\gamma\gamma}$, computed from the two highest p_T photon candidates in an event, is required to be larger than 60 GeV. The azimuthal angle between the two photon candidates, $\Delta\phi_{\gamma\gamma}$, is required to be larger than 0.5, which reduces the background from events where both photon candidates originate from fragmentation, a process that is not well modeled in the simulation, while keeping >97% of the Higgs boson signal for each individual production process.

The selected data sample is contaminated by backgrounds of instrumental origin such as γ + jet (γj), dijet (jj) and $Z/\gamma^* \to e^+e^-$ (ZDY) production, with jets or electrons misidentified as photons, as well as a background from direct $\gamma\gamma$ production (DDP) where two isolated photons are produced. The normalization and shape of the γj and jj backgrounds, as well as the overall normalization of the DDP background, are estimated from data. The Monte Carlo (MC) simulation is used to model the normalization and shape of the signal and ZDY background, as well as the shape of the DDP background. The MC samples used in this analysis are generated using PYTHIA [14] (for signal and ZDY) or SHERPA [15] (for DDP) with CTEQ6L1 [16] parton distribution functions (PDFs), followed by a GEANT-based [17] simulation of the D0 detector. Events from randomly selected beam crossings are overlaid on the simulated events to better model contributions from additional $p\bar{p}$ interactions and detector noise. The same reconstruction algorithms are used as on the data. Signal samples are generated separately for the GF, VH, and VBF processes and normalized using the next-to-next-to-leading order (NNLO) plus next-to-next-to-leading-logarithm (NNLL) theoretical cross sections for GF and NNLO for VH and VBF processes [18–20], computed with the MSTW 2008 PDF set [21]. The Higgs boson's branching ratio predictions are from HDECAY [22]. The ZDY background estimate from MC simulations is normalized to the NNLO cross section [23].

TABLE I. Signal, backgrounds, and data yields for $M_H = 100$ GeV to 150 GeV in 10 GeV intervals within the $[M_H - 30\text{ GeV}, M_H + 30\text{ GeV}]$ mass window. The background yields result from a fit to the data. The uncertainties include both statistical and systematic contributions and take into account correlations among processes. The uncertainty on the total background is smaller than the sum in quadrature of the uncertainties in the individual background sources due to the anticorrelation resulting from the fit.

M_H (GeV)	100	110	120	130	140	150
$\gamma\gamma$ (DDP)	6415 ± 395	4031 ± 286	2779 ± 188	1849 ± 139	1355 ± 99	1026 ± 75
$\gamma j + jj$	5727 ± 352	3819 ± 252	2265 ± 178	1506 ± 120	964 ± 87	641 ± 63
$Z/\gamma^* \to e^+e^-$	599 ± 91	517 ± 81	361 ± 55	141 ± 23	65 ± 12	34 ± 7
Total background	12741 ± 160	8367 ± 134	5405 ± 95	3496 ± 77	2384 ± 57	1701 ± 48
Data	12746	8380	5406	3500	2383	1696
H boson signal	5.9 ± 0.8	5.8 ± 0.8	5.3 ± 0.7	4.2 ± 0.6	2.9 ± 0.4	1.7 ± 0.2
H_f boson signal	149.7 ± 13.2	39.4 ± 3.5	11.9 ± 1.0	4.4 ± 0.4	1.8 ± 0.2	0.7 ± 0.1

The γj and jj yields are estimated with data [24]. Following the final selection, a tightened O_{NN} requirement ($O_{\text{NN}} > 0.75$) is used to classify the events into four categories: (i) both photons, (ii) only the highest p_T (leading) photon, (iii) only the second highest p_T (trailing) photon, or (iv) neither of the two photons, satisfy this requirement. The corresponding numbers of events, after subtracting the ZDY contribution, are denoted as (i) N_{pp}, (ii) N_{pf}, (iii) N_{fp} and (iv) N_{ff}. The different efficiency of the $O_{\text{NN}} > 0.75$ requirement for photons (ϵ_γ) and jets (ϵ_{jet}) is used to estimate the sample composition by solving a linear system of equations:

$$(N_{pp}, N_{pf}, N_{fp}, N_{ff})^T = \mathcal{E} \times (N_{\gamma\gamma}, N_{\gamma j}, N_{j\gamma}, N_{jj})^T,$$

where $N_{\gamma\gamma}$ (N_{jj}) is the number of $\gamma\gamma$ (jj) events and $N_{\gamma j}$ ($N_{j\gamma}$) is the number of γj events with the leading (trailing) cluster as the photon. The 4×4 matrix $\mathcal{E}$ contains the efficiency terms ϵ_γ and ϵ_{jet}, parameterized as a function of $|\eta|$ for each photon candidate and estimated in photon and jet MC samples. We validate ϵ_γ with the data of radiated photon from charged leptons in Z boson decays ($Z \to l^+l^-\gamma$, $l = e, \mu$) and ϵ_{jet} with the jet data [25]. The DDP normalization is determined from a fit to the final discriminant distribution used for hypothesis testing, exploiting the difference in shape between signal and background in each M_H search region. For each M_H hypothesis (between 100 and 150 GeV in steps of 2.5 GeV), the search region is defined to be $M_H \pm 30$ GeV. The shape of the DDP background is obtained from SHERPA [15], while the shapes of the γj and jj backgrounds are obtained from independent data control samples selected by requiring exactly one photon or both photon candidates to satisfy $O_{\text{NN}} < 0.1$, respectively. Table I shows the numbers of data events, expected background, and the expected H boson and H_f boson signals in six of the search regions resulting from a fit described later in this Letter. The estimated background composition is $\approx 48\%$–60% from DDP, $\approx 38\%$–46% from $\gamma j + jj$ and $\approx 2\%$–7% from ZDY, depending on the assumed Higgs boson mass.

To improve the sensitivity of the search, a total of five well-modeled kinematic variables are used to discriminate between signal and background: $M_{\gamma\gamma}$, $\Delta\phi_{\gamma\gamma}$, the transverse momentum of the diphoton system ($p_T^{\gamma\gamma}$), and the transverse momenta of the leading and trailing photons (p_T^1, p_T^2). Figure 1(a) shows a comparison of the $M_{\gamma\gamma}$ distribution between data and the background prediction. Comparisons for other kinematic distributions can be found in Ref. [13]. A boosted-decision-tree (BDT) technique [26] is used to build a single discriminant variable combining

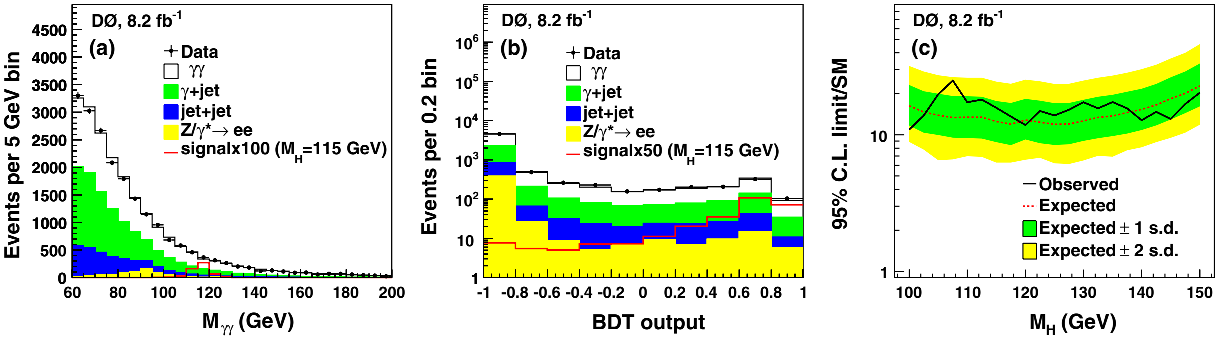

FIG. 1 (color online). (a) $M_{\gamma\gamma}$ and (b) BDT output distributions for $M_H = 115$ GeV after the final selection comparing data to the background prediction. The expected H boson signal is also shown, multiplied by a factor of 100 (a) and 50 (b). (c) Observed and expected 95% C.L. upper limits on $\sigma \times \mathcal{B}$ relative to the SM prediction as a function of M_H. The bands correspond to the ±1 and ±2 standard deviations (s.d.) around the expected limit under the background-only hypothesis.

the information from the above five variables. A different BDT is trained for each M_H hypothesis, separately for the SM and the fermiophobic Higgs boson models. In each model, the training is performed to discriminate between the sum of all relevant signals and the sum of all backgrounds. Figure 1(b) shows a comparison of the BDT output distribution between data and background prediction corresponding to the SM for $M_H = 115$ GeV.

Systematic uncertainties affecting the normalization and shape of the BDT output distribution are estimated for both signal and backgrounds, taking into account correlations. The sources of systematic uncertainties affecting the signal and ZDY background normalizations include the integrated luminosity (6.1%), photon identification efficiency for signal (3.9%) or electron misidentification rate for ZDY (12.7%) and theoretical cross sections (including scale and PDF uncertainties) for signal [GF (14.1%), VH (6.2%), and VBF (4.9%)] and ZDY (3.9%) production. The scale uncertainties are estimated by simultaneously doubling or halving the factorization and renormalization scales. The PDF uncertainty is evaluated according to the prescription of the PDF4LHC group [27]. The normalization uncertainty affecting the $\gamma j + jj$ prediction is 8.4%. This uncertainty results from propagating the uncertainty on the $O_{\rm NN} > 0.75$ efficiency for photons (1.5%) and jets (10%) and also affects the shape of the $\gamma j + jj$ background at the 1%–2% level through changes in the fractions of γj and jj. Additional systematic uncertainties affecting the differential distributions of data and MC simulations include the relative photon energy scale (1%–5% for signal, 1%–4% for DDP), DDP modeling (1%–10%) and Higgs boson p_T modeling in GF (1%–5%). The latter two modeling uncertainties are obtained by doubling and halving the factorization and renormalization scales with respect to the nominal choice.

No evidence for a signal, either in the SM or in the fermiophobic interpretations, is found, and the BDT discriminants are used to derive upper limits on the production cross section multiplied by the branching ratio for $H \rightarrow \gamma\gamma$ ($\sigma \times \mathcal{B}$) as a function of M_H. Limits are calculated at the 95% C.L. with the CL_S modified frequentist approach using a log-likelihood ratio of the signal-plus-background ($S + B$) hypothesis to the background-only (B) hypothesis [28]. Systematic uncertainties are taken into account by convoluting the Poisson probability distributions for signal and background with the corresponding Gaussian distributions. The individual likelihoods are maximized with respect to the DDP background normalization as well as parameters that describe the systematic uncertainties [29]. This fit allows the determination of the normalization for the DDP background from data and significantly reduces the impact of systematic uncertainties on the overall sensitivity.

The resulting upper limits on $\sigma \times \mathcal{B}$ relative to the SM prediction as a function of M_H are shown in Fig. 1(c), representing the most constraining results for a SM Higgs boson decaying into photons. Upper limits on $\mathcal{B}(H_f \rightarrow \gamma\gamma)$ as a function of M_{H_f} are presented in Fig. 2 and compared to the combined LEP result [30], using the same model as in the present Letter. The sensitivity is improved by about a factor of 2 relative to previous searches at the Tevatron [7], yielding the most stringent limits on a fermiophobic Higgs boson of $M_{H_f} > 112.9$ GeV at 95% C.L.

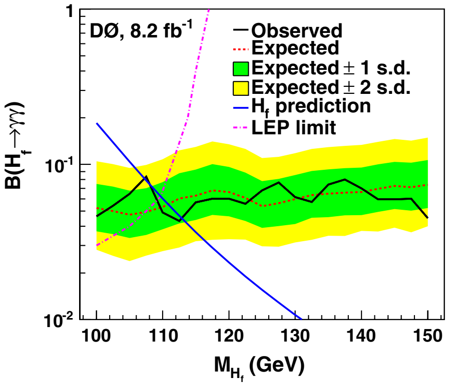

FIG. 2 (color online). Observed and expected 95% C.L. upper limits on $\mathcal{B}(H_f \rightarrow \gamma\gamma)$ as a function of M_{H_f}. The definition of the bands are the same as in Fig. 1(c). The blue line represents the branching ratio predictions from HDECAY [22]. Also displayed is the combined exclusion region obtained by the LEP Collaborations [30], using the same model as in the present Letter.

We thank the staffs at Fermilab and collaborating institutions, and acknowledge support from the DOE and NSF (USA); CEA and CNRS/IN2P3 (France); FASI, Rosatom and RFBR (Russia); CNPq, FAPERJ, FAPESP and FUNDUNESP (Brazil); DAE and DST (India); Colciencias (Colombia); CONACyT (Mexico); KRF and KOSEF (Korea); CONICET and UBACyT (Argentina); FOM (The Netherlands); STFC and the Royal Society (United Kingdom); MSMT and GACR (Czech Republic); CRC Program and NSERC (Canada); BMBF and DFG (Germany); SFI (Ireland); The Swedish Research Council (Sweden); and CAS and CNSF (China).

---

[*] Deceased.

[†] Visitor from Augustana College, Sioux Falls, SD, USA.

[‡] Visitor from The University of Liverpool, Liverpool, UK.

[§] Visitor from SLAC, Menlo Park, CA, USA.

[||] Visitor from University College London, London, UK.

[¶] Visitor from Centro de Investigacion en Computacion-IPN, Mexico City, Mexico.

[**] Visitor from ECFM, Universidad Autonoma de Sinaloa, Culiacán, Mexico.

[††] Visitor from Universität Bern, Bern, Switzerland.

[1] R. Barate *et al.* (LEP Working Group for Higgs Boson Searches), Phys. Lett. B **565**, 61 (2003).
[2] LEP, Tevatron ad SLD Electroweak Working Groups, arXiv:1012.2367.
[3] T. Aaltonen *et al.* (CDF and D0 Collaboration), Phys. Rev. Lett. **104**, 061802 (2010); Tevatron New Phenomena and Higgs Working Group, arXiv:1103.3233.
[4] B. Holdom *et al.*, PMC Phys. A **3**, 4 (2009).
[5] S. Mrenna and J. Wells, Phys. Rev. D **63**, 015006 (2000).
[6] V. M. Abazov *et al.* (D0 Collaboration), Phys. Rev. Lett. **102**, 231801 (2009).
[7] T. Affolder *et al.* (CDF Collaboration), Phys. Rev. Lett. **103**, 061803 (2009); V. M. Abazov *et al.* (D0 Collaboration), Phys. Rev. Lett. **101**, 051801 (2008).
[8] V. M. Abazov *et al.* (D0 Collaboration), Nucl. Instrum. Methods Phys. Res., Sect. A **565**, 463 (2006); M. Abolins *et al.* (D0 Collaboration), Nucl. Instrum. Methods Phys. Res., Sect. A **584**, 75 (2008); R. Angstadt *et al.* (D0 Collaboration), Nucl. Instrum. Methods Phys. Res., Sect. A **622**, 298 (2010).
[9] Pseudorapidity is defined as $\eta = -\ln[\tan(\theta/2)]$, where θ is the polar angle relative to the proton beam direction and ϕ is the azimuthal angle in the plane transverse to the proton beam direction.
[10] T. Andeen *et al.*, Report No. FERMILAB-TM-2365, 2007.
[11] X. Bu, FERMILAB-THESIS-2010-29, 2010.
[12] V. M. Abazov *et al.* (D0 Collaboration), Phys. Lett. B **659**, 856 (2008).
[13] See Supplemental Material at http://link.aps.org/supplemental/10.1103/PhysRevLett.107.151801 for details on the photon neural network and on comparisons of data and MC simulations for the BDT input variables.
[14] T. Sjöstrand *et al.*, J. High Energy Phys. 05 (2006) 026. Version 6.409 was used.
[15] T. Gleisberg *et al.*, J. High Energy Phys. 02 (2009) 007. Version 1.2.2 was used.
[16] J. Pumplin *et al.*, J. High Energy Phys. 07 (2002) 012; D. Stump *et al.*, J. High Energy Phys. 10 (2003) 046.
[17] R. Brun and F. Carminati, CERN Program Library Long Writeup W5013, 1993.
[18] C. Anastasiou, R. Boughezal, and F. Petriello, J. High Energy Phys. 04 (2009) 003; D. Florian and M. Grazzini, Phys. Lett. B **674**, 291 (2009).
[19] J. Baglio and A. Djouadi, J. High Energy Phys. 10 (2010) 064.
[20] P. Bolzoni, F. Maltoni, S.-O. Moch, and M. Zaro, Phys. Rev. Lett. **105**, 011801 (2010).
[21] A. D. Martin, W. J. Stirling, R. S. Thorne, and G. Watt, Eur. Phys. J. C **63**, 189 (2009).
[22] A. Djouadi, J. Kalinowski, and M. Spira, Comput. Phys. Commun. **108**, 56 (1998). Version 3.70 was used.
[23] R. Hamberg, W. L. van Neerven, and T. Matsuura, Nucl. Phys. B **359**, 343 (1991); **644**, 403(E) (2002).
[24] D. Acosta *et al.* (CDF Collaboration), Phys. Rev. Lett. **95**, 022003 (2005).
[25] V. M. Abazov *et al.* (D0 Collaboration), Phys. Lett. B **690**, 108 (2010).
[26] A. Hoecker *et al.*, Proc. Sci., ACAT (2007) 040 [arXiv:physics/0703039].
[27] S. Alekhin, S. Alioli, R. D. Ball and *et al.*, arXiv:1101.0536; M. Botje, J. Butterworth, and A. Cooper-Sarkar *et al.*, arXiv:1101.0538.
[28] T. Junk, Nucl. Instrum. Methods Phys. Res., Sect. A **434**, 435 (1999); A. Read, J. Phys. G **28**, 2693 (2002).
[29] W. Fisher, FERMILAB-TM-2386-E (2006).
[30] A. Heister *et al.* (ALEPH Collaboration), Phys. Lett. B **544**, 16 (2002); P. Abreu *et al.* (DELPHI Collaboration), Eur. Phys. J. C **35**, 313 (2004); P. Achard *et al.* (L3 Collaboration), Phys. Lett. B **568**, 191 (2003); G. Abbiendi *et al.* (OPAL Collaboration), Phys. Lett. B **544**, 259 (2002); A. Rosca (LEP Collaborations), Nucl. Phys. B, Proc. Suppl. **117**, 743 (2003).